

## **Modeling of Density-Dependent Flow and Transport in Anisotropic Aquifers: An Example Site of Landfill**

JIAN-SHUH JEAN<sup>1</sup>, and FENG-SUEY CHEN<sup>1</sup>

(Manuscript received 28 May 1994, in final form 30 December 1994)

### **ABSTRACT**

**In advection-dispersion transport processes, the density contrast between the contaminant fluid and the groundwater in the surrounding flow domain can affect the groundwater flow. Under such circumstances, the migration patterns and concentration distributions of contaminant plumes can be changed. The primary purpose of this research is to simulate the problems of density-dependent groundwater flow and transport in homogeneous, anisotropic and inhomogeneous (or heterogeneous), anisotropic aquifers by means of a Galerkin finite element method. Secondly, this research is to show the numerical model of Galeati *et al.* (1992) can be applied to a landfill site.**

**The leachate from a landfill site into the groundwater can change the contaminant concentration. Thus, there exists a density contrast between the contaminant fluid and the groundwater in the surrounding flow domain. In simulation, an example site of landfill is demonstrated. The results for contaminant sources from a landfill conclude as follows. If there does not exist a significant density contrast, the contaminant plume will spread in a shallow zone close to the water table; on the other hand, if there is such a contrast, the plume will sink downward into the groundwater flow system, and its migration pattern will only be changed after a longer transport time of six years. In a shorter time (one to three years), however, the migration pattern will not be significantly changed.**

**(Key words: Density-dependent flow and transport, Modeling, Landfill)**

### **1. INTRODUCTION**

In advection-dispersion transport processes, the migration pattern of the contaminant plume resulting from the leachate in a landfill site is influenced by many factors, including (1) the density contrast (or density difference ratio) between the contaminant or tracer fluid and the groundwater in the surrounding flow domain, (2) the groundwater flow velocity and direction, (3) the input history of the contaminant (e.g. injected velocity and concentration),

---

<sup>1</sup> Department of Earth Sciences, National Cheng Kung University, Tainan, Taiwan, R.O.C.

(4) the dispersivity, and (5) the aquifer properties (e.g., porosity, storage, hydraulic conductivity contrasts of aquifer materials, etc.). This research provides a more accurate prediction of the migration pattern of a contaminant plume based on the causative factors mentioned above. In determining the depth and location of monitoring wells for groundwater quality, an accurate prediction of migration patterns in the vertical and horizontal section coordinates  $(x, z)$  and  $(x, y)$  in the modeling solute transport is required.

In the published literature, most density-dependent solute transport models have considered seawater intrusion into an aquifer (e.g., Henry, 1964; Segol *et al.*, 1975; Kuiper, 1983; Voss and Souza, 1987; Huyakorn *et al.* 1987; Dorgarten and Tsang, 1991; and Galeati *et al.*, 1992). Frind (1982) applied the seawater intrusion concept to simulate the solute transport of leachate resulting from a landfill site. Freeze and Cherry (1979) indicated that if the contaminant solution entering the flow regime has the same density as the groundwater, the contaminant plume will spread in a shallow zone close to the water table. If the contaminant solution is considerably denser than the groundwater, the plume will sink downward into the groundwater system.

Recently, Galeati *et al.* (1992) provided a more advanced continuity equation based on different assumptions for the fluid from the one by Frind (1982). However, Galeati *et al.* (1992) applied their model of density-dependent transport to seawater intrusion into an aquifer, not to a landfill site. This research simulates the problems of density-dependent groundwater flow and transport in homogeneous, anisotropic and inhomogeneous, anisotropic aquifers for a landfill site by means of a Galerkin finite element method. An example site of landfill is demonstrated for simulation. The purpose of this research is to show the numerical model of Galeati *et al.* (1992) is applicable to a landfill site.

## 2. CONTINUITY EQUATIONS OF FLUID AND SOLUTE

### 2.1 Fluid Continuity Equation

The continuity equation for the unsteady-state fluid used in this research is the same as that used for the problem of seawater intrusion by Galeati *et al.* (1992). It is written as:

$$\frac{\partial}{\partial x_i} \left[ K_{ij} \left( \frac{\partial h}{\partial x_j} + \gamma C \eta_j \right) \right] = S_s \frac{\partial h}{\partial t} + \frac{\phi \rho_0 \gamma}{\rho} \frac{\partial C}{\partial t} - Q. \quad (1)$$

Equation (1) by Galeati *et al.* (1992) is more advanced than the one by Frind (1982). The second term on the right side of (1) which is due to the time derivative of the liquid density does not exist in the equation by Frind (1982).

With the density contrast (or density difference ratio) defined as:

$$\gamma = \frac{\rho_{\max} - \rho_0}{\rho_0}, \quad (2)$$

the constitutive relation is written as:

$$\rho = \rho_0(1 + \gamma C), \quad (3)$$

where  $K_{ij}$  is the hydraulic conductivity tensor,  $x_j$  ( $j=1,2,3$ ) are Cartesian coordinates (with 1 and 2 standing for the horizontal and 3 for the vertical directions),  $h$  is the hydraulic head,

$\eta_j$  is a vector such that  $\eta_j=0$  along the horizontal direction and  $\eta_j=1$  along the vertical,  $\gamma$  is the density contrast (or density difference ratio),  $S_s$  is the specific storage,  $t$  is the time,  $\phi$  is the porosity,  $Q$  is a fluid source term,  $\rho_0$  freshwater density,  $\rho_{\max}$  is the density corresponding to the maximum concentration, and  $C$  is a dimensionless concentration (actual divided by maximum). In (1), it is assumed that the conditions are isothermal, the fluid is incompressible and the salt does not undergo chemical reactions. It is also assumed that its concentration is not high enough to affect viscosity or to invalidate Darcy's and Fick's laws (Hassanizadeh and Leijnse, 1988).

The flow equation is taken to satisfy initial and boundary conditions. For the initial condition:

$$h(x_i, t) = h_0(x_i) \quad t = 0, \quad (4)$$

where  $h_0$  is the initial equivalent head. For the condition on the Dirichlet boundaries  $\Gamma_1$ :

$$h(x_i, t) = \bar{h}(x_i, t) \quad t > 0, \quad (5)$$

where  $\bar{h}$  is the prescribed head. For the condition on the Neumann boundaries  $\Gamma_2$ :

$$q_n = -U_i n_i = q_0(x_i, t) \quad t > 0, \quad (6)$$

where  $q_0$  is the prescribed fluid flux normal to the boundaries  $\Gamma_2$  (positive inward), and  $U_i$  is the Darcy flux given by:

$$U_i = -K_{ij} \left( \frac{\partial h}{\partial x_j} + \gamma C \eta_j \right). \quad (7)$$

For the condition on the boundaries  $\Gamma_3$  (combination of the Dirichlet and Neumann boundaries):

$$h(x_i, t) = h(x_i, t) \quad t > 0$$

$$q_n = -U_i n_i = q_0(x_i, t) \quad t > 0. \quad (8)$$

## 2.2 Solute Continuity Equation

The solute continuity equation is expressed as:

$$\frac{\partial}{\partial x_i} \left( \phi D_{ij} \frac{\partial C}{\partial x_j} \right) - \frac{\partial}{\partial x_i} (U_i C) = \phi \frac{\partial C}{\partial t} - C^* Q \quad (\text{Bear, 1979}), \quad (9)$$

$$\text{and } C^* = C_k \text{ for injection; } C^* = C_s \text{ for abstraction,} \quad (10)$$

where  $C_k$  and  $C_s$  are the relative concentrations of the solute injected and pumped with the fluid sources, respectively, and  $D_{ij}$  is the dispersion tensor which is defined as in Galeati *et al.* (1992).

The solute transport equation is taken to satisfy the initial condition:

$$C(x_i, t) = C_0(x_i) \quad t = 0, \quad (11)$$

where  $C_0$  is the initial concentration. For the condition on the Dirichlet boundaries  $\Gamma_1$ :

$$C(x_i, t) = \bar{C}(x_i, t) \quad t > 0, \quad (12)$$

where  $\bar{C}$  is the prescribed concentration. For the condition on the Neumann boundaries  $\Gamma_2$ :

$$\phi D_{ij} \frac{\partial C}{\partial x_j} n_i = q^d(x_i, t) \quad t > 0, \quad (13)$$

where  $q^d$  is the prescribed dispersive flux normal to the boundaries  $\Gamma_2$  (positive inward). For the condition on the Cauchy or Robin boundaries  $\Gamma_3$ :

$$\left( U_i C - \phi D_{ij} \frac{\partial C}{\partial x_j} \right) n_i = q^c(x_i, t) \quad t > 0, \quad (14)$$

where  $q^c$  is the prescribed flux of concentration across the boundaries.

### 3. GALERKIN FINITE ELEMENT SOLUTIONS

The numerical formulations used below to solve density-dependent flow and transport in a landfill site follow the Galerkin finite element method.

#### 3.1 Fluid Flow Equation

Recalling (1) for the continuity equation of the fluid, a two-dimensional system of coordinates  $(x, z)$  which does not necessarily coincide with the principal axes of the conductivity tensor can be written as:

$$\begin{aligned} \frac{\partial}{\partial x} \left[ K_{xx} \frac{\partial h}{\partial x} \right] + \frac{\partial}{\partial x} \left[ K_{xz} \left( \frac{\partial h}{\partial z} + \gamma C \right) \right] + \frac{\partial}{\partial z} \left[ K_{zx} \frac{\partial h}{\partial x} \right] + \\ \frac{\partial}{\partial z} \left[ K_{zz} \left( \frac{\partial h}{\partial z} + \gamma C \right) \right] = S_s \frac{\partial h}{\partial t} + \frac{\phi \rho_0 \gamma}{\rho} \frac{\partial C}{\partial t} - Q. \end{aligned} \quad (15)$$

In the Galerkin weighting procedure, the trial solution  $\hat{h}$  is first defined to approximate the solution and  $h$  is represented by  $\hat{h}$  such that:

$$h \cong \hat{h} = \sum N h = N_i h_i + N_j h_j + N_m h_m + N_n h_n, \quad (16)$$

where  $i, j, m, n$  are nodal points for each rectangular element, and  $N$  is the basis or weighting function. The residuals  $R(\hat{h})$  are then defined in terms of trial heads as:

$$\begin{aligned}
 R(\hat{h}) = & \frac{\partial}{\partial x} \left[ K_{xx} \frac{\partial \hat{h}}{\partial x} \right] + \frac{\partial}{\partial x} \left[ K_{xz} \left( \frac{\partial \hat{h}}{\partial z} + \gamma C \right) \right] + \frac{\partial}{\partial z} \left[ K_{zx} \frac{\partial \hat{h}}{\partial x} \right] + \\
 & \frac{\partial}{\partial z} \left[ K_{zz} \left( \frac{\partial \hat{h}}{\partial z} + \gamma C \right) \right] - S_s \frac{\partial \hat{h}}{\partial t} - \frac{\phi \rho_0 \gamma}{\rho} \frac{\partial C}{\partial t} + Q.
 \end{aligned} \quad (17)$$

Substituting the approximate solution (16) into (17), and setting the resulting residuals orthogonal to all the basis functions  $N_L$  over the flow domain  $A$ :

$$\int \int_A R(\hat{h}) N_L dx dz = 0 \quad L = 1, 2, \dots, n \quad n = \text{total number of nodes.} \quad (18)$$

Applying Green's identity to (17) and (18) and rearranging yields:

$$\begin{aligned}
 & \int \int_A \left[ K_{xx} \frac{\partial \hat{h}}{\partial x} \frac{\partial N_L}{\partial x} + K_{xz} \left( \frac{\partial \hat{h}}{\partial z} + \gamma C \right) \frac{\partial N_L}{\partial x} + K_{zx} \frac{\partial \hat{h}}{\partial x} \frac{\partial N_L}{\partial z} \right. \\
 & \quad \left. + K_{zz} \left( \frac{\partial \hat{h}}{\partial z} + \gamma C \right) \frac{\partial N_L}{\partial z} \right] dx dz + \int \int_A S_s \frac{\partial \hat{h}}{\partial t} N_L dx dz + \\
 & \int \int_A \frac{\phi \rho_0 \gamma}{\rho} \frac{\partial C^m}{\partial t} N_L dx dz - \int \int_A Q N_L dx dz = \int_{\Gamma} \left[ K_{xx} \frac{\partial \hat{h}}{\partial x} n_x \right. \\
 & \quad \left. + K_{xz} \left( \frac{\partial \hat{h}}{\partial z} + \gamma C \right) n_x + K_{zx} \frac{\partial \hat{h}}{\partial x} n_z + K_{zz} \left( \frac{\partial \hat{h}}{\partial z} + \gamma C \right) n_z \right] N_L d\Gamma, \quad (19)
 \end{aligned}$$

where  $N_L$  is the basis function at  $L=1,2,\dots,n$  nodal points,  $n_x$  and  $n_z$  are  $x$  and  $z$  components of unit vector outward and normal to the boundaries, and  $C^m$  is the mean concentration over an element. For the sake of simplicity,  $C$  is taken to represent the spatial average within each element (Galeati, et al., 1992). Subdividing the whole domain  $A$  for (19) into  $N$  rectangular elements and substituting (16) into (19) yields:

$$\begin{aligned}
 & \sum_{e=1}^N \int \int_e \left[ \left( K_{xx} \frac{\partial N_i}{\partial x} \frac{\partial N_L}{\partial x} + K_{xz} \frac{\partial N_i}{\partial z} \frac{\partial N_L}{\partial x} + K_{zx} \frac{\partial N_i}{\partial x} \frac{\partial N_L}{\partial z} + K_{zz} \frac{\partial N_i}{\partial z} \frac{\partial N_L}{\partial z} \right) h_i \right. \\
 & \quad \left. + \left( K_{xx} \frac{\partial N_j}{\partial x} \frac{\partial N_L}{\partial x} + K_{xz} \frac{\partial N_j}{\partial z} \frac{\partial N_L}{\partial x} + K_{zx} \frac{\partial N_j}{\partial x} \frac{\partial N_L}{\partial z} + K_{zz} \frac{\partial N_j}{\partial z} \frac{\partial N_L}{\partial z} \right) h_j \right]
 \end{aligned}$$

$$\begin{aligned}
& + (K_{xx} \frac{\partial N_m}{\partial x} \frac{\partial N_L}{\partial x} + K_{xz} \frac{\partial N_m}{\partial z} \frac{\partial N_L}{\partial x} + K_{zx} \frac{\partial N_m}{\partial x} \frac{\partial N_L}{\partial z} + K_{zz} \frac{\partial N_m}{\partial z} \frac{\partial N_L}{\partial z}) h_m \\
& + (K_{xx} \frac{\partial N_n}{\partial x} \frac{\partial N_L}{\partial x} + K_{xz} \frac{\partial N_n}{\partial z} \frac{\partial N_L}{\partial x} + K_{zx} \frac{\partial N_n}{\partial x} \frac{\partial N_L}{\partial z} + K_{zz} \frac{\partial N_n}{\partial z} \frac{\partial N_L}{\partial z}) h_n \Big] dx dz \\
& + \sum_{e=1}^N \int \int_e \gamma C (K_{xz} \frac{\partial N_L}{\partial x} + K_{zz} \frac{\partial N_L}{\partial z}) dx dz + \sum_{e=1}^N \int \int_e S_s (N_i N_L \frac{\partial h_i}{\partial t} + \\
& \quad N_j N_L \frac{\partial h_j}{\partial t} + N_m N_L \frac{\partial h_m}{\partial t} + N_n N_L \frac{\partial h_n}{\partial t}) dx dz + \\
& \sum_{e=1}^N \int \int_e \frac{\phi \rho_0 \gamma}{\rho} \frac{\partial C^m}{\partial t} N_L dx dz - \int \int_e Q N_L dx dz = \sum_{e=1}^N \int_{\Gamma} \left[ K_{xx} \frac{\partial \hat{h}}{\partial x} n_x \right. \\
& \quad \left. + K_{xz} (\frac{\partial \hat{h}}{\partial z} + \gamma C) n_x + K_{zx} \frac{\partial \hat{h}}{\partial x} n_z + K_{zz} (\frac{\partial \hat{h}}{\partial z} + \gamma C) n_x \right] N_L d\Gamma, \quad (20)
\end{aligned}$$

where  $\sum_{e=1}^N$  indicates the summation over the  $N$  elements. Equation (20) is a Galerkin finite element scheme for flow in inhomogeneous, anisotropic media and is written in matrix form as:

$$[G]\{h\} + \{\gamma C\} + [S_s] \left\{ \frac{\partial h}{\partial t} \right\} + \left[ \frac{\phi \rho_0 \gamma}{\rho} \right] \left\{ \frac{\partial C^m}{\partial t} \right\} - \{Q\} = \{q_0\}, \quad (21)$$

where  $[G]$  is the conductance matrix,  $\{\gamma C\}$  is the body force vector,  $[S_s]$  is the fluid mass matrix,  $\left[ \frac{\phi \rho_0 \gamma}{\rho} \right]$  is the porosity matrix with the body force,  $\{Q\}$  is the fluid source vector, and  $\{q_0\}$  is the boundary flux vector. The use of the implicit finite difference form to solve the time derivative term in (21) yields:

$$[G]\{h^{t+\Delta t}\} + \{\gamma C\} + [S_s] \left\{ \frac{h^{t+\Delta t} - h^t}{\Delta t} \right\} + \left[ \frac{\phi \rho_0 \gamma}{\rho} \right] \left\{ \frac{C_{new}^m - C_{old}^m}{\Delta t} \right\} - \{Q\} = \{q_0\}. \quad (22)$$

Rearranging (22) yields:

$$\begin{aligned}
& \left\{ [G] + \frac{1}{\Delta t} [S_s] \right\} \{h\}^{t+\Delta t} - \frac{1}{\Delta t} [S_s] \{h\}^t + \{\gamma C\} + \\
& \left[ \frac{\phi \rho_0 \gamma}{\rho} \right] \left\{ \frac{C_{new}^m - C_{old}^m}{\Delta t} \right\} - \{Q\} = \{q_0\}. \quad (23)
\end{aligned}$$

The above equation can be used to numerically solve the head value for each nodal point in inhomogeneous, anisotropic media.

### 3.2 Point Velocity

To avoid discontinuity across the boundary between two elements, the flow velocity for each nodal point in inhomogeneous, anisotropic media is solved from Yeh (1981) by:

$$\begin{aligned} R_x &= \hat{q}_x + K_{xx} \frac{\partial \hat{h}}{\partial x} + K_{xz} \left( \frac{\partial \hat{h}}{\partial z} + \gamma C \right) \\ R_z &= \hat{q}_z + K_{zz} \left( \frac{\partial \hat{h}}{\partial z} + \gamma C \right) + K_{zx} \frac{\partial \hat{h}}{\partial x}, \end{aligned} \quad (24)$$

where  $R_x$ ,  $R_z$  are residuals at  $x$ ,  $z$  components, and  $\hat{q}_x$ ,  $\hat{q}_z$  are trial solutions of Darcy velocities at  $x$ ,  $z$  directions. With the resulting residuals set orthogonal to all the basis functions,  $N_L$  over the flow domain  $A$  yields:

$$\int \int_A \left[ \hat{q}_x + K_{xx} \frac{\partial \hat{h}}{\partial x} + K_{xz} \left( \frac{\partial \hat{h}}{\partial z} + \gamma C \right) \right] N_L dx dz = 0 \quad L = 1, 2, \dots, n,$$

$n$  = total number of nodes

$$\text{or} \quad \int \int_A \left[ \hat{q}_x N_L + K_{xx} \frac{\partial \hat{h}}{\partial x} N_L + K_{xz} \left( \frac{\partial \hat{h}}{\partial z} + \gamma C \right) \right] N_L dx dz = 0. \quad (25)$$

$\hat{q}_z$  can be achieved in a similar fashion. Substituting the trial solution  $\hat{h}$  in (16) into (25) and subdividing the whole domain into  $N$  rectangular elements yields:

$$\begin{aligned} & \sum_{e=1}^N \int \int_e (N_i N_L q_{x_i} + N_j N_L q_{x_j} + N_m N_L q_{x_m} + N_n N_L q_{x_n}) dx dz = \\ & - \sum_{e=1}^N \int \int_e \left[ (K_{xx} \frac{\partial N_i}{\partial x} N_L + K_{xz} \frac{\partial N_i}{\partial z} N_L) h_i + (K_{xx} \frac{\partial N_j}{\partial x} N_L + K_{xz} \frac{\partial N_j}{\partial z} N_L) h_j \right. \\ & \left. + (K_{xx} \frac{\partial N_m}{\partial x} N_L + K_{xz} \frac{\partial N_m}{\partial z} N_L) h_m + (K_{xx} \frac{\partial N_n}{\partial x} N_L + K_{xz} \frac{\partial N_n}{\partial z} N_L) h_n \right] dx dz \\ & - \sum_{e=1}^N \int \int_e K_{xz} \gamma (N_L C_i + N_L C_j + N_L C_m + N_L C_n) dx dz. \end{aligned} \quad (26)$$

Equation (26) can be written in matrix form as:

$$[N]\{q\} = -[k]\{h\} - [K\gamma]\{C\}, \quad (27)$$

where  $[N]$  is the basis function matrix,  $[K]$  is the hydraulic conductivity matrix, and  $[K\gamma]$  is the hydraulic conductivity (at  $x, z$  coordinates) matrix with the density contrast. Therefore, the flow velocity for each nodal point in inhomogeneous, anisotropic media can be found.

### 3.3 Solute Transport Equation

It should be recalled that the solute continuity equation is expressed as:

$$\begin{aligned} & \left( \phi D_{xx} \frac{\partial^2 C}{\partial x^2} + \phi D_{xz} \frac{\partial^2 C}{\partial x \partial z} + \phi D_{zx} \frac{\partial^2 C}{\partial z \partial x} + \phi D_{zz} \frac{\partial^2 C}{\partial z^2} \right) - \left( U_x \frac{\partial C}{\partial x} + U_z \frac{\partial C}{\partial z} \right) \\ & = \phi \frac{\partial C}{\partial t} - C^* Q \quad (\text{Bear, 1979}), \end{aligned} \quad (28)$$

where  $C^* = C_k$  for injection and  $C^* = C_s$  for abstraction.  $C_k$  and  $C_s$  are as defined before. It is to be noted that  $D_{xx}$ ,  $D_{xz}$ ,  $D_{zx}$  and  $D_{zz}$  are allowed to vary in space.  $U_x$  and  $U_z$ , the Darcy fluxes, are assumed to be constant in space since the density differences as used in this research were small, and  $\frac{\partial U_x}{\partial x}$  and  $\frac{\partial U_z}{\partial z} = 0$ . If the density differences were high,  $\frac{\partial U_x}{\partial x}$  and  $\frac{\partial U_z}{\partial z}$  can not be ignored, and hence,  $U_x$  and  $U_z$  are not constant in space. The procedure for the Galerkin finite element scheme in (28) can be achieved in a similar fashion. The trial solution  $\hat{C}$  is first defined to approximate the solution  $C$  such that:

$$C \cong \hat{C} = \sum N C = N_i C_i + N_j C_j + N_m C_m + N_n C_n, \quad (29)$$

where  $C$  is the concentration. The residuals  $R(\hat{C})$  are defined in terms of concentrations as:

$$\begin{aligned} R(\hat{C}) = & \left( \phi D_{xx} \frac{\partial^2 \hat{C}}{\partial x^2} + \phi D_{xz} \frac{\partial^2 \hat{C}}{\partial x \partial z} + \phi D_{zx} \frac{\partial^2 \hat{C}}{\partial z \partial x} + \phi D_{zz} \frac{\partial^2 \hat{C}}{\partial z^2} \right) \\ & - \left( U_x \frac{\partial \hat{C}}{\partial x} + U_z \frac{\partial \hat{C}}{\partial z} \right) - \phi \frac{\partial \hat{C}}{\partial t} + C^* Q. \end{aligned} \quad (30)$$

With the approximate solution (29) substituted into (30), and the resulting residuals set orthogonal to all basis functions  $N_L$  over the flow domain  $A$ :

$$\int \int_A R(\hat{C}) N_L dx dy = 0 \quad L = 1, 2, \dots, n \quad n = \text{total number of nodes.} \quad (31)$$

Applying Green's identity to (30)-(31) and replacing  $\hat{C}^*$  by  $\hat{C}$  yields:

$$\begin{aligned}
 & - \int \int_A \left( \phi D_{xx} \frac{\partial \hat{C}}{\partial x} \frac{\partial N_L}{\partial x} + \phi D_{xz} \frac{\partial \hat{C}}{\partial z} \frac{\partial N_L}{\partial x} + \phi D_{zx} \frac{\partial \hat{C}}{\partial x} \frac{\partial N_L}{\partial z} + \phi D_{zz} \frac{\partial \hat{C}}{\partial z} \frac{\partial N_L}{\partial z} \right) dx dz \\
 & - \int \int_A \left( U_x \frac{\partial \hat{C}}{\partial x} + U_z \frac{\partial \hat{C}}{\partial z} \right) N_L dx dz - \int \int_A \phi \frac{\partial \hat{C}}{\partial t} N_L dx dz + \int \int_A \hat{C} Q N_L dx dz \\
 & + \int_{\Gamma} \left( \phi D_{xx} \frac{\partial \hat{C}}{\partial x} + \phi D_{xz} \frac{\partial \hat{C}}{\partial z} n_x + \phi D_{zx} \frac{\partial \hat{C}}{\partial x} n_z + \phi D_{zz} \frac{\partial \hat{C}}{\partial z} \right) N_L d\Gamma = 0. \quad (32)
 \end{aligned}$$

The Galerkin finite element scheme for solute transport in inhomogeneous, anisotropic media is similar to that of the fluid flow equation and can be written in matrix form as:

$$\begin{aligned}
 & [G]\{C\} + [U]\{C\} + [P] \left\{ \frac{\partial C}{\partial t} \right\} - [QN]\{C\} = [UN]\{C\} - \{q_0 C_0\}, \\
 \text{or} \quad & [G]\{C^{t+\Delta t}\} + [U]\{C^{t+\Delta t}\} + [P] \left\{ \frac{C^{t+\Delta t} - C^t}{\Delta t} \right\} \\
 & - [QN]\{C^{t+\Delta t}\} - [UN]\{C^{t+\Delta t}\} + \{q_0 C_0\} = 0, \quad (33)
 \end{aligned}$$

where  $[G]$  is the conductance matrix,  $[U]$  is the matrix of the average Darcy velocity for each element,  $[P]$  is the basis function matrix with porosity,  $[QN]$  is the fluid source matrix,  $[UN]$  is the boundary Darcy velocity matrix, and  $\{q_0 C_0\}$  is the boundary flux vector. From (33), the solute concentration or relative concentration for each nodal point in inhomogeneous, anisotropic media can then be found.

#### 4. COMPARISONS WITH MASS BALANCE CALCULATIONS AND PUBLISHED RESULTS

Since the analytical equation for (1) by Galeati *et al.* (1992) has not yet been refined in this research isochlors published by Frind (1982) for leachate transport are compared with those of Galeati *et al.* (1992), recalling that the governing equation of Frind (1982) does not include the second term as shown in equation (1).

Additionally, the mass balance error was used to evaluate the accuracy of the numerical solution. The mass balance error can be expressed by:

$$\begin{aligned}
 & [\text{Net material flux across the whole boundary}] \\
 & + [\text{net rate of mass production owing to well pumping or injection}] \\
 & - [\text{rate of mass storage}] = 0 \quad (34)
 \end{aligned}$$

Equations (9) or (28) can be written as:

$$\int_{\Gamma} \left( \phi D \frac{\partial \hat{C}}{\partial l} \right) N_L n_L d\Gamma + \int \int_A Q C^* N_L dx dz - \int \int_A \frac{\partial \hat{C}}{\partial t} N_L dx dz = 0, \quad (35)$$

where  $QC^*$  is the net rate of mass production owing to well pumping or injection, and  $\hat{C}$  is the trial solution of the concentration. For the Cauchy boundaries:

$$\phi D \frac{\partial \hat{C}}{\partial l} = \phi U \hat{C} - q_0 C_0. \quad (36)$$

For the Neumann boundaries:

$$\phi D \frac{\partial \hat{C}}{\partial l} = -q_0 C_0. \quad (37)$$

For the Dirichlet boundaries:

$$\phi D \frac{\partial \hat{C}}{\partial l} = \phi U \hat{C}. \quad (38)$$

Let:

$$\begin{aligned} F_{b_i} &= \int_{\Gamma} \left( \phi D \frac{\partial \hat{C}}{\partial l} \right) N_L n_i d\Gamma \\ F_{Q_i} &= \int \int_A QC^* N_L dx dz \\ F_{d_i} &= \int \int_A \frac{\partial \hat{C}}{\partial t} N_L dx dz. \end{aligned} \quad (39)$$

Equation (35) can be written as:

$$\varepsilon = \sum_{i=1}^{n_b} F_{b_i} + \sum_{i=1}^{n_Q} F_{Q_i} + \sum_{i=1}^{n_d} F_{d_i}, \quad (40)$$

where  $\varepsilon$  is the rate of mass loss,  $n_b$  is the number of nodes on the whole boundary,  $n_Q$  is the number of pumping and/or injection wells, and  $n_d$  is the total number of nodes in the whole solution region. Thus, the mass balance error (E) used as an indicator of the accuracy of the numerical solution of the transport equation is expressed as:

$$E = \sum_{p=1}^k \left[ \frac{(\varepsilon \Delta t)^P}{\Delta t (\sum_{i=1}^{n_b} |F_{b_i}| + \sum_{i=1}^{n_Q} |F_{Q_i}| + \sum_{i=1}^{n_d} |F_{d_i}|)} \right], \quad (41)$$

where  $p$  is the time level, and  $k$  is the cumulative time level. The mass balance errors shown in the simulation results are computed from equation (41).

Figure 1 represents the leachate solute transport in a landfill disposal site and concerns a homogeneous, anisotropic unconfined aquifer bounded on the left and right by constant head and concentration boundaries, on the bottom by an impermeable boundary, on the top

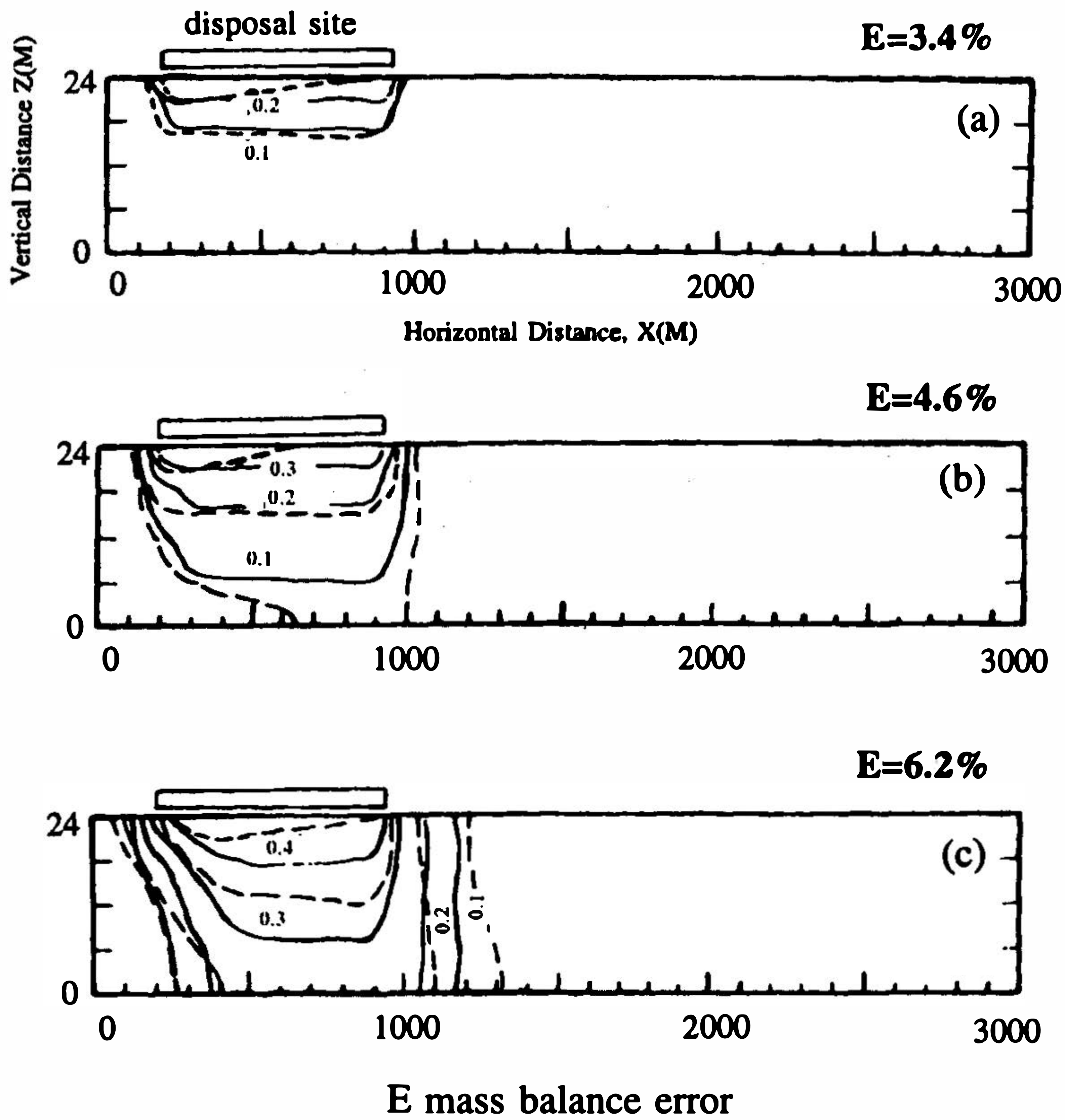


Fig. 1. Isochlors for leachate transport problem by this research (solid lines) compared to conditions and results of Frind (1982) (dashed lines): (a) 1.5 years, (b) 3 years, (c) 6 years of elapsed time.

by a specified flow boundary ( $q=30$  cm/year), with the solute flux at the contaminant source by the Cauchy boundaries and the initial input concentration of one ( $C_0=1$ ). The concentration is initially zero, and the freshwater heads steadily in accordance with the specified boundary conditions. With reference to Figure 1, the configurations of the boundaries and the system parameters adopted for the numerical simulation are as follows:

Configurations: Top boundary  $q_z = q_0$ ,  $\frac{q_z}{\phi} C - D_{zz} \frac{\partial C}{\partial z} = q_0 C_0$ ; bottom boundary  $q=0$ ,  $\frac{\partial C}{\partial z}=0$ ; left boundary  $h=h_0$ ,  $C=0$ ; right boundary  $h=h_L$ ,  $C=0$

Parameters:  $K_{xx}=32 \times 10^{-4}$  m/sec,  $K_{zz}=3.2 \times 10^{-5}$  m/sec;  $S_s=10^{-4}$  m<sup>-1</sup>;  $\phi=0.2$ ;  $h_0=0.0$  m,  $h_L=-17.5$  m;  $\alpha_L=10$  m,  $\alpha_T=1$  m;  $\rho_r=\gamma C=0.0071$ ;  $q_0=30$  cm/year;  $C_0=0$ ,  $0 \leq x \leq x_1$ ;  $C_0=1$ ,  $x_1 \leq x \leq x_2$ ;  $C_0=0$ ,  $x_2 \leq x \leq x_L$ ;  $X_L=3000$  m,  $x_1=120$  m,  $x_2=920$  m,  $z_H=24$  m

In the simulation of this case, 275 rectangular elements and 216 nodes were used;  $\Delta t$  was allowed to increase gradually by a factor of 1.2 from 0.0001 to 100 days. Figure 1 shows that the modeling results of isochlors at the transport times of 1.5, 3, and 6 years computed

by Frind (1982) (in dashed lines) and this research (in solid lines) are in fair agreement. The concentration distributions at 1.5 years of Figure 1(a) with a 3.4% mass balance error (E) agree with those by Frind (1982). However, the position of 0.1 isochlor at 3 years by Frind (1982) has migrated to the aquifer bottom, but not in Figure 1(b) from this research with a 4.6% mass balance error. This implies that the solute transport at 3 years according to Frind (1982) is faster than that in this research. The concentration distributions by Frind (1982) at a transport time of 6 years, however, agree with those of Figure 1(c) in this research with a 6.2% mass balance error. This indicates that the solute transport after a long time in this study and by Frind (1982) are in good agreement. The governing equation for fluid flow by Galeati *et al.* (1992) as in equation (1) is mostly updated and more advanced than that used by Frind (1982). Therefore, equation (1) is used to model solute transport from a landfill in this research.

## 5. SIMULATION RESULTS

The validation of the model in this research on homogeneous, anisotropic and inhomogeneous (heterogeneous), anisotropic aquifers allows for its application to other cases of interest. The following scenarios are for modeling leachate solute transport in wedge-shaped aquifers in landfill disposal sites.

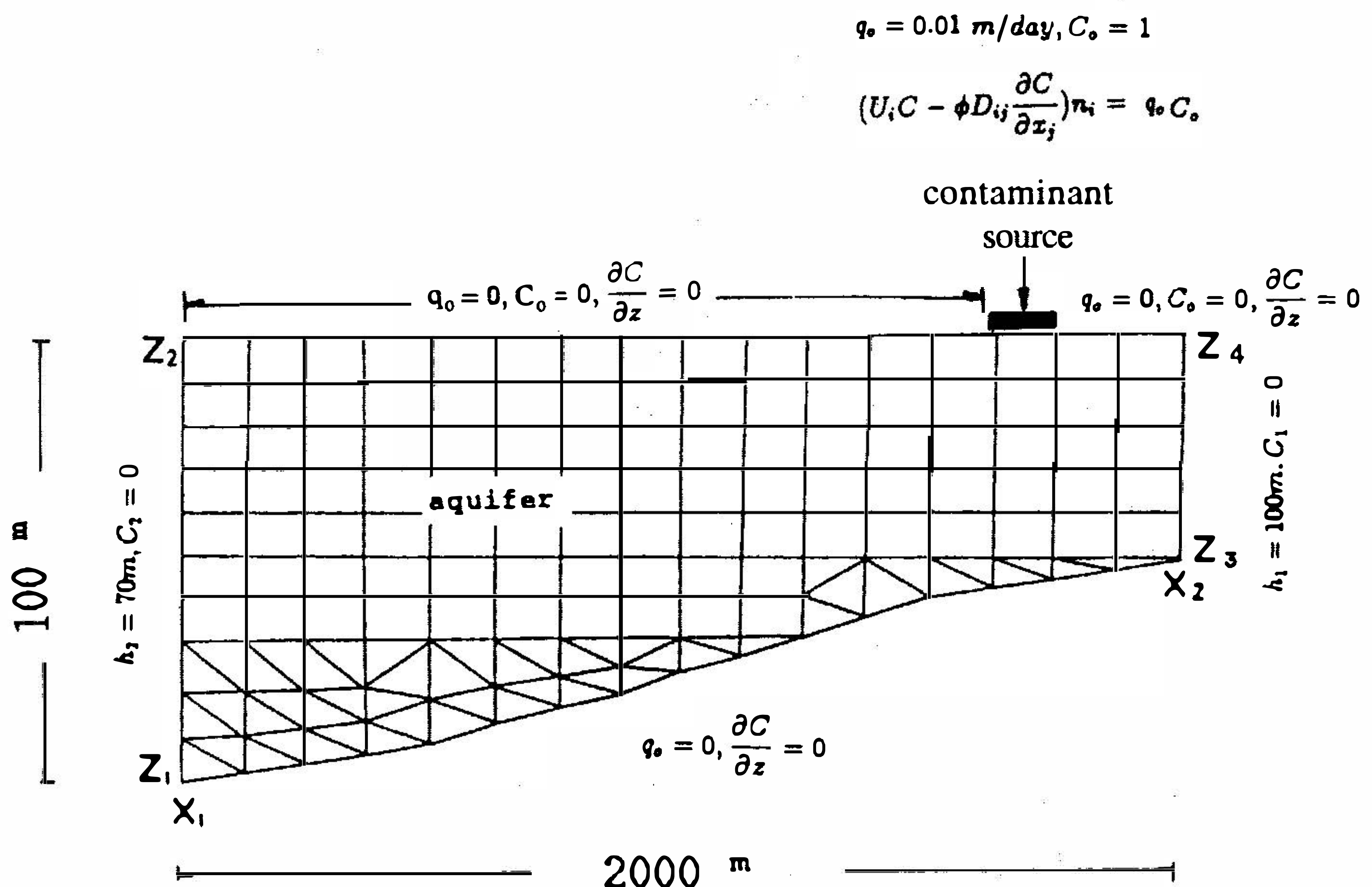


Fig.2. Boundary conditions and finite element discretizations for modeling leachate transport in a homogeneous, anisotropic wedge-shaped unconfined aquifer (modified from Huyakorn *et al.*, 1985).

### 5.1 Case 1: Homogeneous, Anisotropic Unconfined Aquifer

This scenario concerns an aquifer bounded as per the example in Figure 1 but with the specified flow boundary  $q_0=0.01$  m/day. The concentration is initially zero, and the freshwater heads steadily in accordance with the specified boundary conditions. The hydrogeologic and

boundary conditions, the configuration of the boundaries, the finite element discretizations in Figure 2 as well as the system parameters adopted for the numerical simulation are:

|                    |  |
|--------------------|--|
| bottom boundary    | $q_0=0, \frac{\partial C}{\partial z}=0$   |
| top boundary       | $q_0=0.01$ m/day, $C_0=1$ for $1625 \text{ m} \leq x \leq 1750 \text{ m}$ ,<br>and $q_0=0, C_0=0, \frac{\partial C}{\partial z}=0$ for $x > 1750 \text{ m}$ and $x < 1625 \text{ m}$   |
| right boundary     | $h_1=100 \text{ m}, C_1=0$   |
| left boundary      | $h_2=70 \text{ m}, C_2=0$  |
| aquifer properties | $K_{xx}=10$ m/day, $K_{zz}=5$ m/day, $K_{xz}=K_{zx}=2$ m/day,<br>$\alpha_L=60$ m (longitudinal dispersivity),<br>$\alpha_T=5$ m (transverse dispersivity),<br>$\phi=0.25, S_y=0.01$ (specific yield),<br>$D_d=0$ (molecular diffusion) |

In the simulation in this scenario, 100 rectangular and 53 triangular elements plus 151 nodes were used;  $\Delta t$  was allowed to increase gradually by a factor of 1.25 from 0.0001 to 100 days. Figure 3 shows concentrations at the transport times of 1, 3 and 6 years without density-dependent flow ( $\gamma=0$ ). The 0.13 concentration lines in (a,b,c) of Figure 3 have not yet migrated to the aquifer bottom. Now it should be assumed that the density contrast ( $\gamma$ ) between the contaminant and the groundwater is 0.004. Figure 4 shows the concentrations at transport times of 1, 3, and 6 years with an approximate mass balance error of 2.0%. Figures 4(a,b) and 3(a,b) show no changes in the concentration distribution at the transport times of 1 and 3 years. However, the concentration of 0.13 at the transport time of 6 year, as shown in Figure 4(c), has reached the bottom of the wedge-shaped aquifer, but not in Figure 3(c). When the density contrast increases to 0.007 ( $\gamma=0.007$ ), the concentration of 0.16 at the transport time of 6 years has nearly reached the bottom as shown in Figure 5(c). From the comparisons of the concentration distributions shown above, it becomes evident that the concentration distributions after the short-time transport of one year show no significant difference. However, when the transport time increases to six years, the concentration distribution and migration pattern of the contaminant plume obviously change. It is especially true that when the contaminant solution is denser than the groundwater, the plume sinks downward into the groundwater flow system and disperses away from the contaminant source.

## 5.2 Case2: Inhomogeneous, Anisotropic Unconfined Aquifer

This scenario concerns an inhomogeneous, anisotropic wedge-shaped unconfined aquifer with an aquitard lens. The finite element discretizations are shown in Figure 6. The boundary conditions and system parameters, except for the aquitard lens, are the same as those in Case 1, and the system parameters for the lens adopted for the numerical simulation are:

$$K_{xx}=0.02 \text{ m/day}, K_{zz}=0.02 \text{ m/day},$$

$$K_{xz}=K_{zx}=0,$$

$$\alpha_L=30 \text{ m (longitudinal dispersivity)},$$

$$\alpha_T=2 \text{ m (transverse dispersivity)},$$

$\phi=0.45$ ,  $S_y=0.02$  (specific yield),

$D_d = 0$  (molecular diffusion)

The modeling results of solute transport at 1, 3, and 6 years are shown in Figure 7, and they show that the contaminant can migrate through the aquitard lens, but its concentration contours are distorted, especially at 3 and 6 years (Figures 7b, 7c). This indicates the transport migration pattern can also be influenced by the hydraulic conductivity contrast between different geologic materials. The hydraulic conductivity of the aquifer and aquitard materials are hundred to one, i.e., two orders of magnitude different. With differences of more than two orders of magnitude in hydraulic conductivity, the transport migration pattern can be affected.

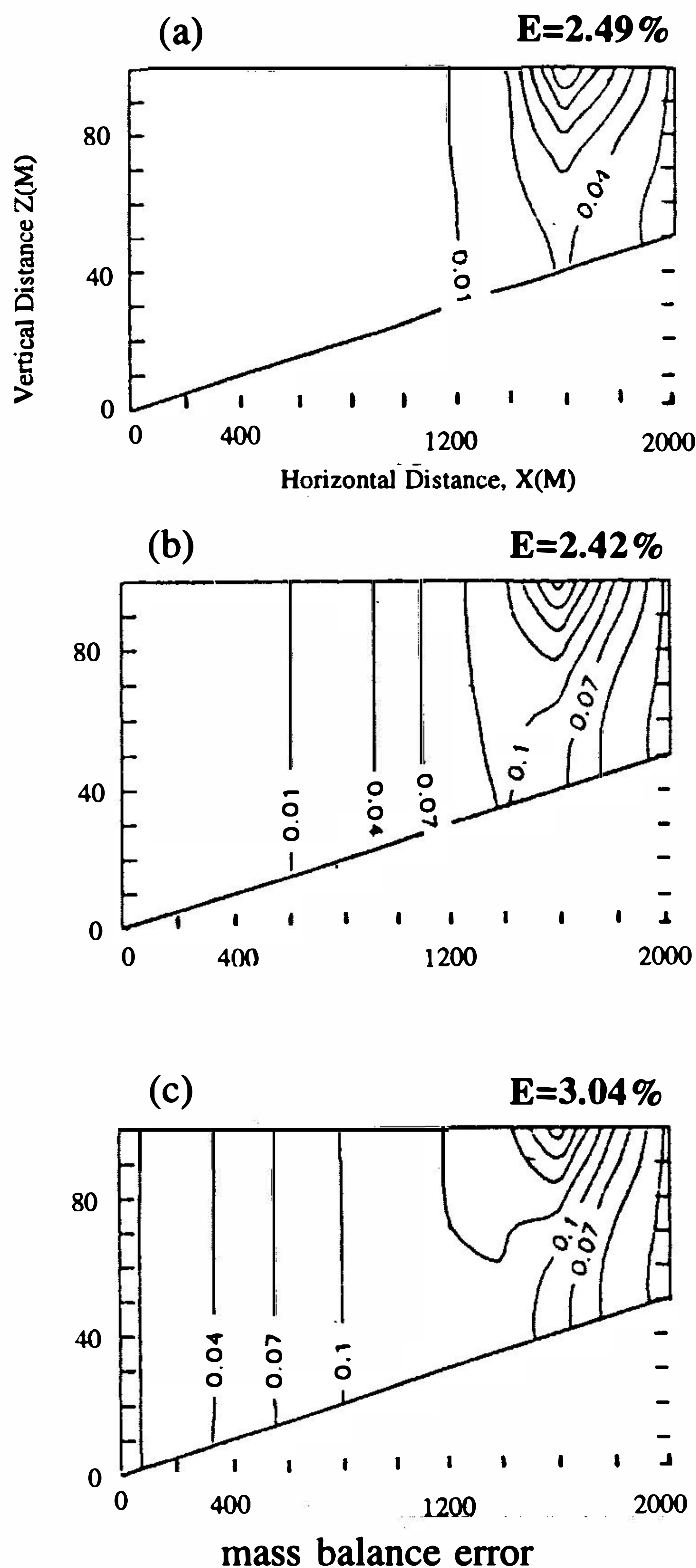


Fig.3. Concentration distributions for modeling leachate transport in a homogeneous, anisotropic wedge-shaped unconfined aquifer after: (a) 1 year, (b) 3 years, (c) 6 years of elapsed time with the density contrast  $\gamma = 0$ .

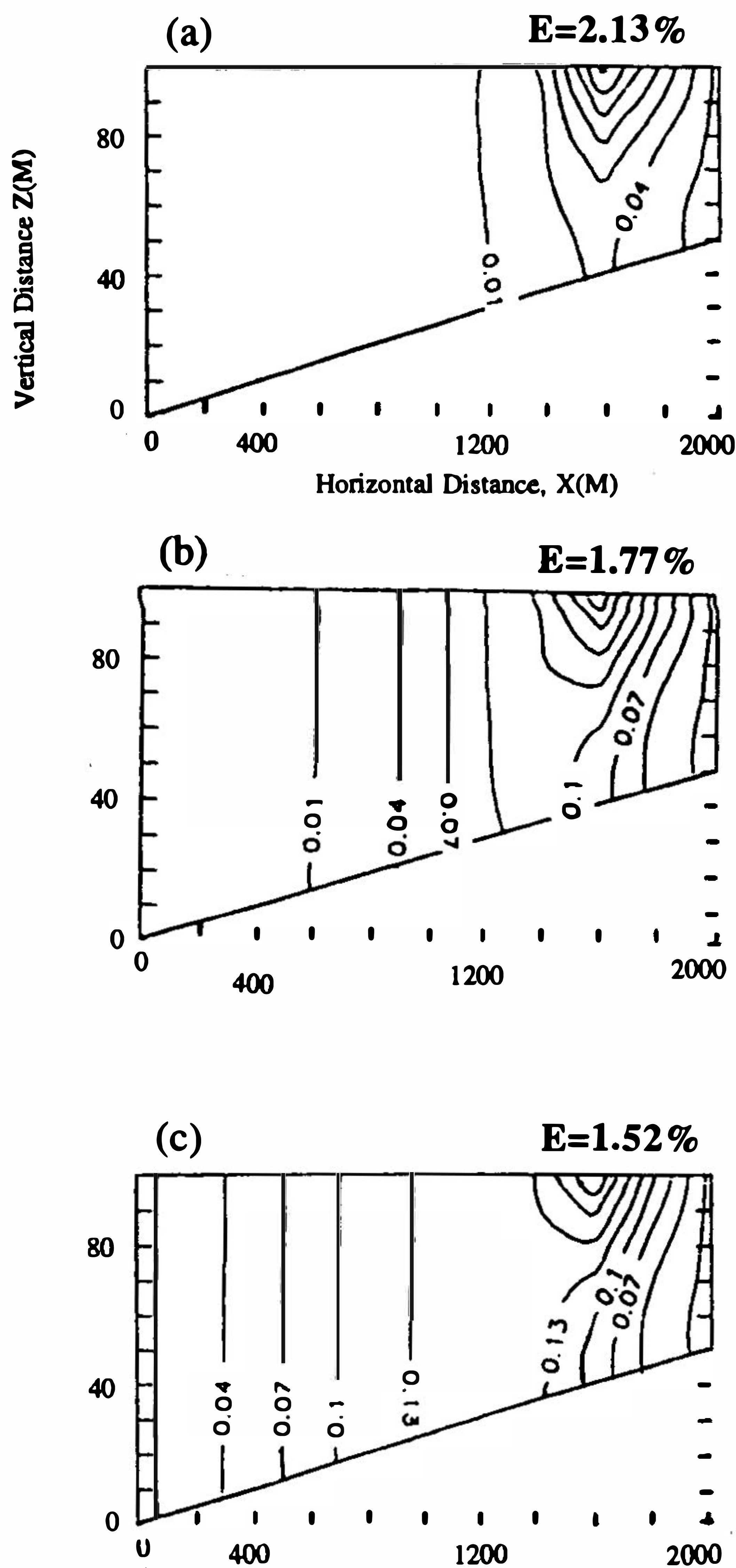


Fig.4. Concentration distributions for modeling leachate transport in a homogeneous, anisotropic wedge-shaped unconfined aquifer after: (a) 1 year, (b) 3 years, (c) 6 years of elapsed time with the density contrast  $\gamma=0.004$ .

### 5.3 Example Site of Landfill

The numerical model was used for application in a practical way to a certain landfill in Taiwan. Figure 8 shows the site along with the location of its boreholes. The B-B' geological section was made as shown in Figure 9, and the hydrogeologic conditions and boundaries for the numerical simulation are known. The whole profile of the site from bottom to top is grey silty clay, grey silty sand or sandy silt (aquifer 2), grey silty clay occasionally with fine sand inclusion, and brown silty fine sand (aquifer 1). The hydrogeologic condition of this site is a homogeneous and anisotropic unconfined aquifer (i.e., aquifer 1), which is underlain by an homogeneous, isotropic aquitard and a homogeneous, anisotropic confined aquifer (aquifer



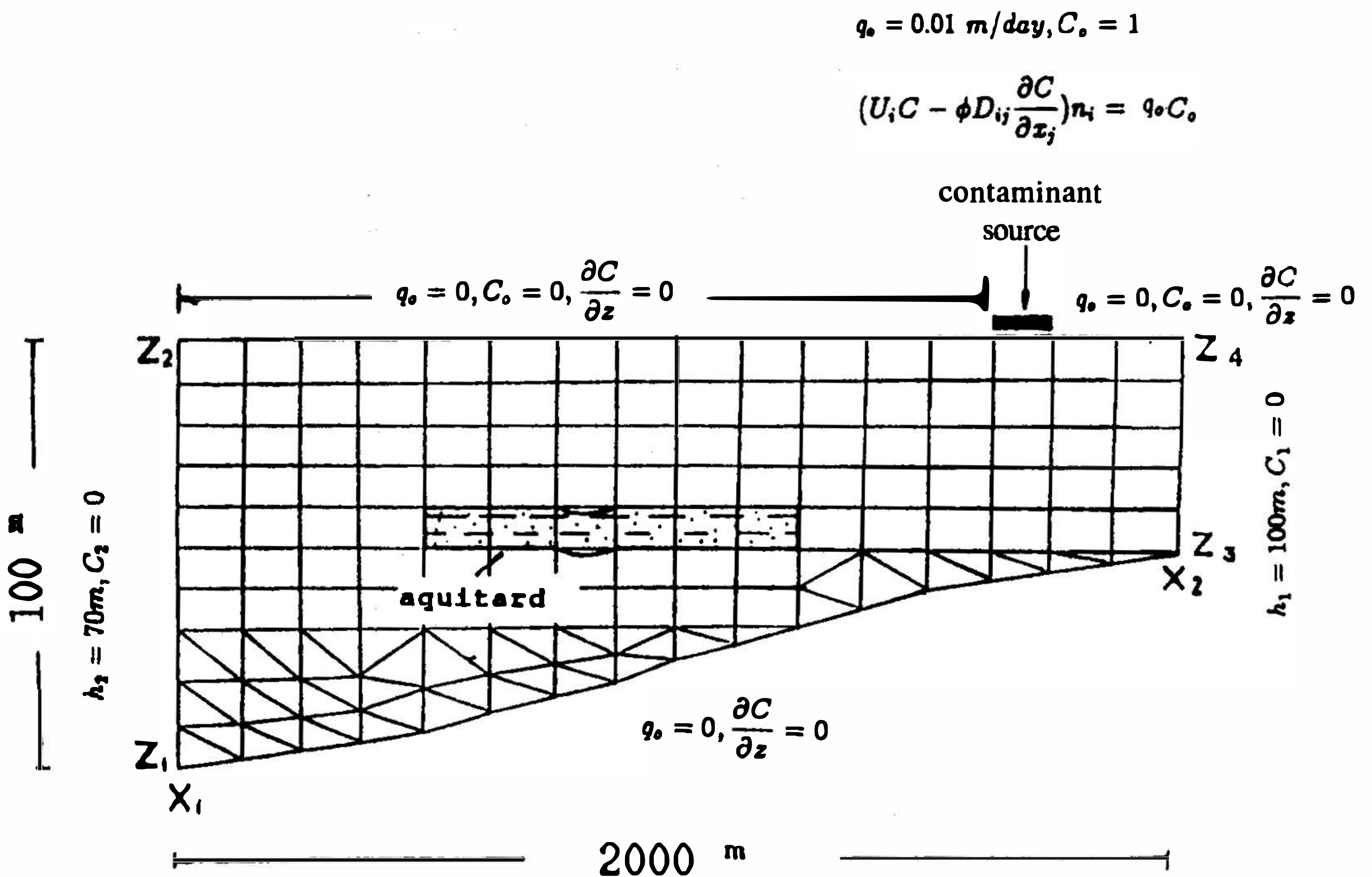


Fig. 6. Boundary conditions and finite element discretizations for modeling leachate transport in an inhomogeneous, anisotropic wedge-shaped unconfined aquifer (modified from Huyakorn *et al.* 1985).

left  $h_1=14 \text{ m}, C_1=0$

right  $h_2=10 \text{ m}, C_2=0$

$x_1=0, x_2=800 \text{ m}, z_1=0 \text{ m}, z_2=22 \text{ m}, z_3=0 \text{ m}, z_4=10 \text{ m}$

Physical parameters:

aquifer 1:  $K_{xz}=15 \text{ m/day}, K_{zz}=5 \text{ m/day}, K_{xz}=K_{zx}=0 \text{ m/day}, \alpha_L=50 \text{ m}, \alpha_T=5 \text{ m},$

$D_d=0, \phi=0.3, R_d=1$  (retardation factor)

aquitard:  $K_{xx}=0.03 \text{ m/day}, K_{zz}=0.03 \text{ m/day}, K_{xz}=K_{zx}=0 \text{ m/day}, \alpha_L=30 \text{ m}, \alpha_T=2 \text{ m},$

$D_d=0, \phi=0.5, R_d=1$  (retardation factor)

aquifer 2:  $K_{xx}=15 \text{ m/day}, K_{zz}=5 \text{ m/day}, K_{xz}=K_{zx}=0 \text{ m/day}, \alpha_L=50 \text{ m}, \alpha_T=5 \text{ m},$

$D_d=0, \phi=0.3, R_d=1$  (retardation factor)

The boundary conditions and finite element discretizations consisting of 89 rectangular elements and 26 triangular elements and 125 nodal points are shown in Figure 10.

In simulation, the time interval  $\Delta t$  was allowed to increase gradually by a factor of 1.25 from 0.001 to 100 days. The equipotential lines and flow lines for a steady-state flow in the confined aquifer are shown in Figure 11 (a). The ground water flow direction is from left to right, and thus, the leachate contaminant plume is moved to the right. The concentration distributions after a 1000-day (2.7 years) and a 2000-day (5.5 years) transport with the density contrast of  $\gamma=0.0071$  are shown in Figures 11(b) and (c), respectively. In

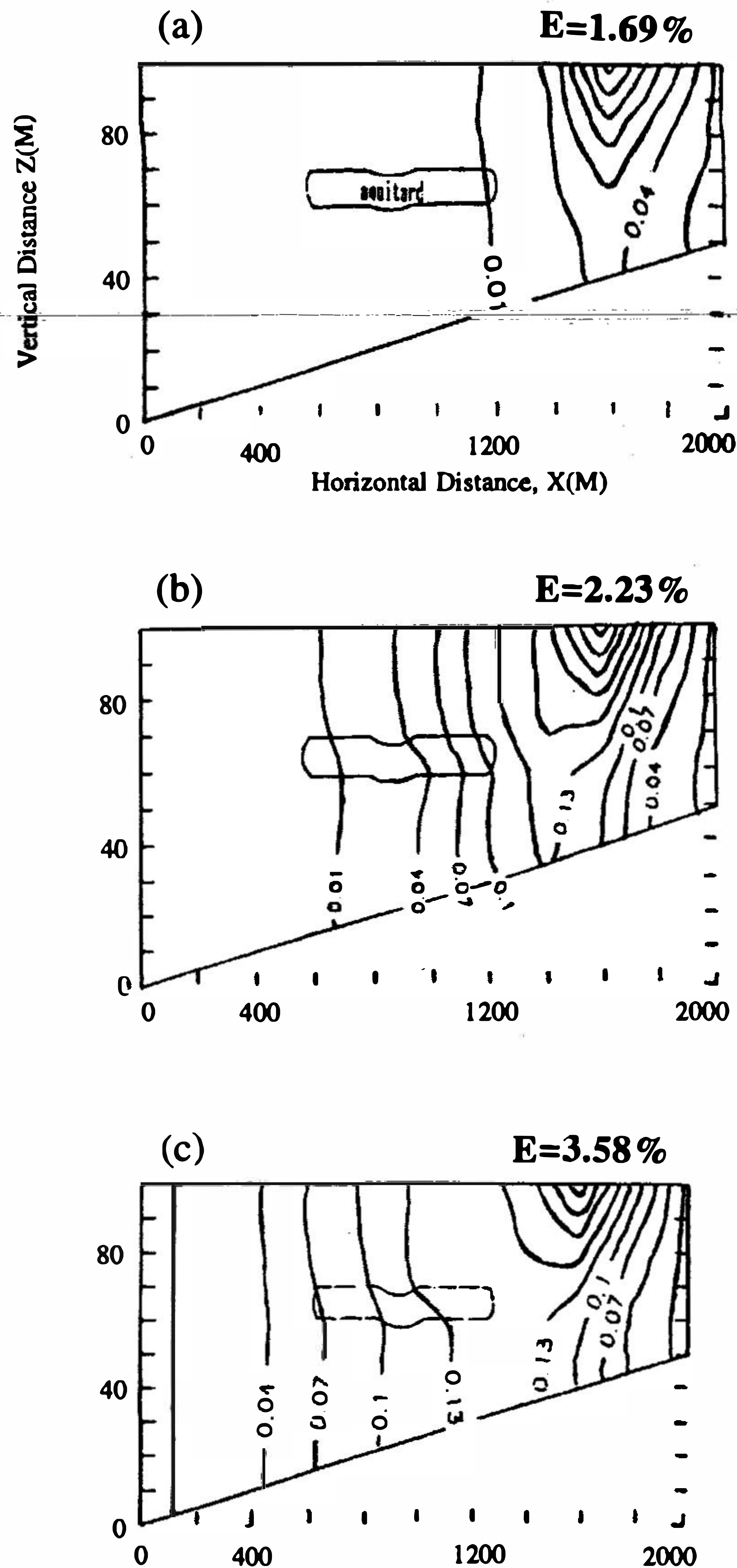


Fig.7. Concentration distributions for modeling leachate transport in an inhomogeneous, anisotropic wedge-shaped aquifer after: (a) 1 year, (b) 3 years, (c) 6 years of elapsed time with the density contrast  $\gamma=0.007$ .

comparison, the plume after a 2000-day transport as in Figure 11(c) spreads more in the horizontal direction than after a 1000-day transport as in Figure 11(b). The plume after a 2000-day transport has percolated and reached the confined aquifer (i.e., aquifer 2), but not in the case of the 1000-day transport. This demonstrates that the contaminant plume sinks downward into the groundwater flow system in aquifer 2 after a longer transport time of 2000 days if the density contrast between the contaminant fluid and the groundwater is more significant (i.e.,  $\gamma=0.0071$ ). This means that the migration pattern of the plume is changed due to the density effect.

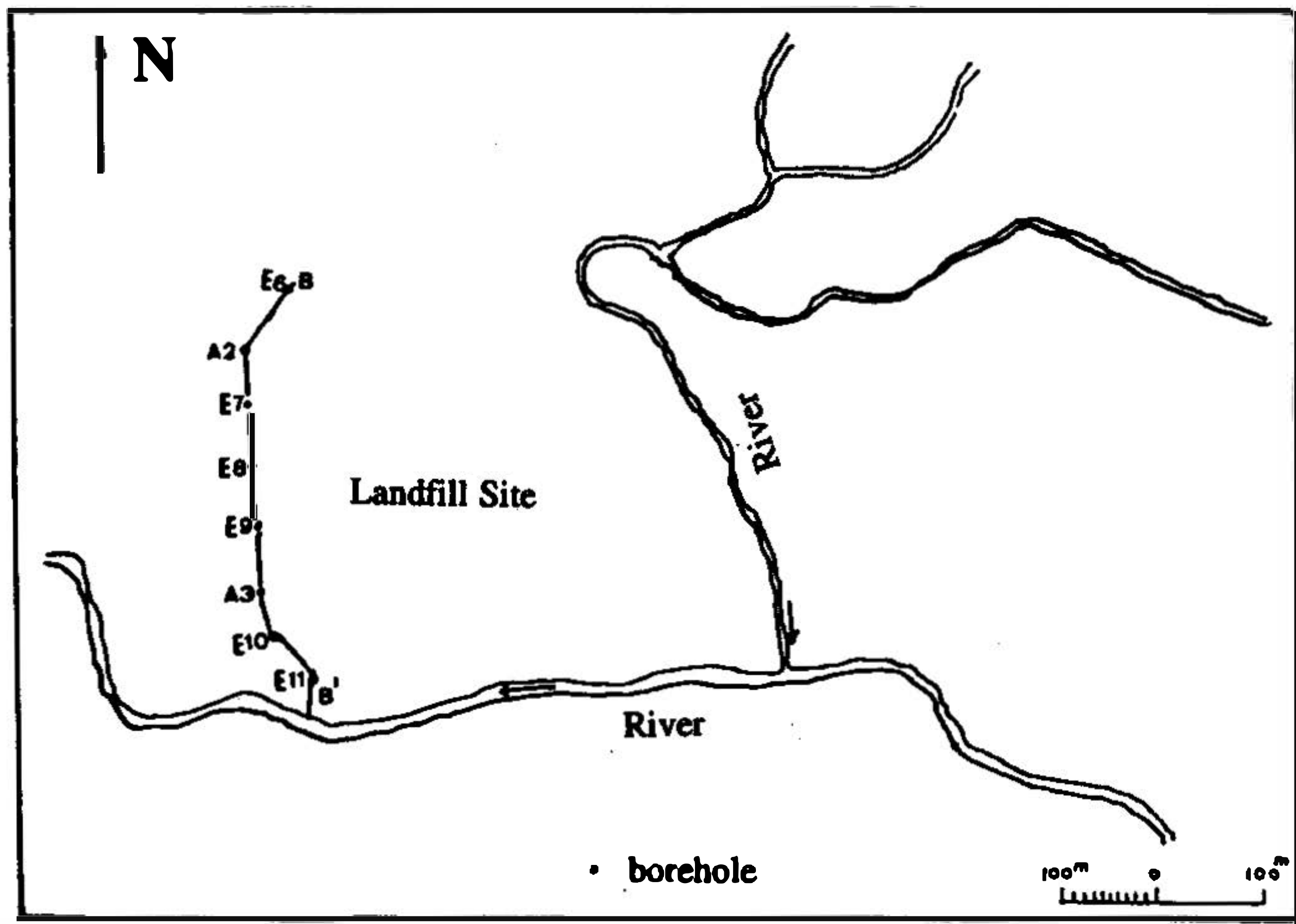


Fig. 8. Location of the example site of a certain landfill.

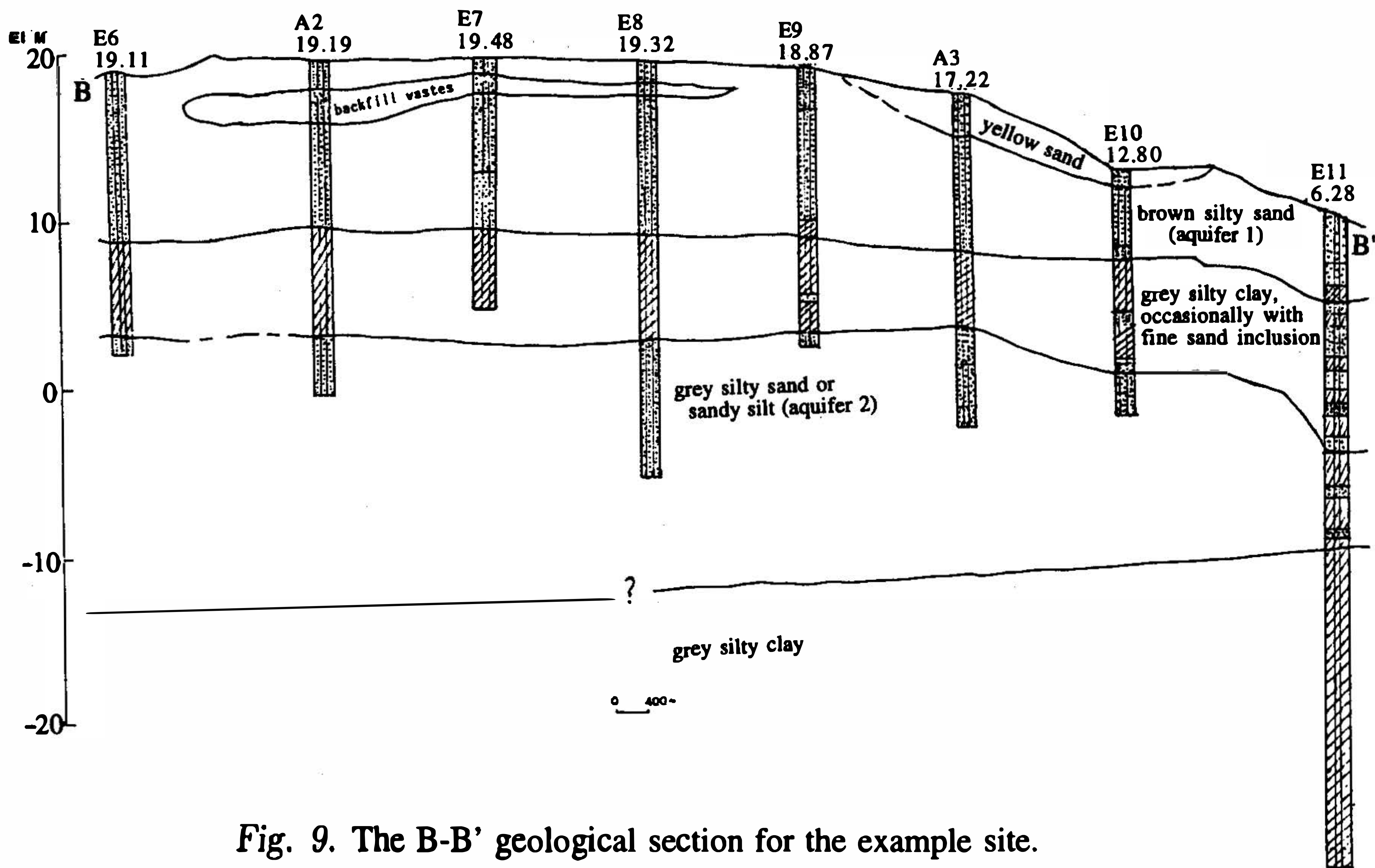


Fig. 9. The B-B' geological section for the example site.

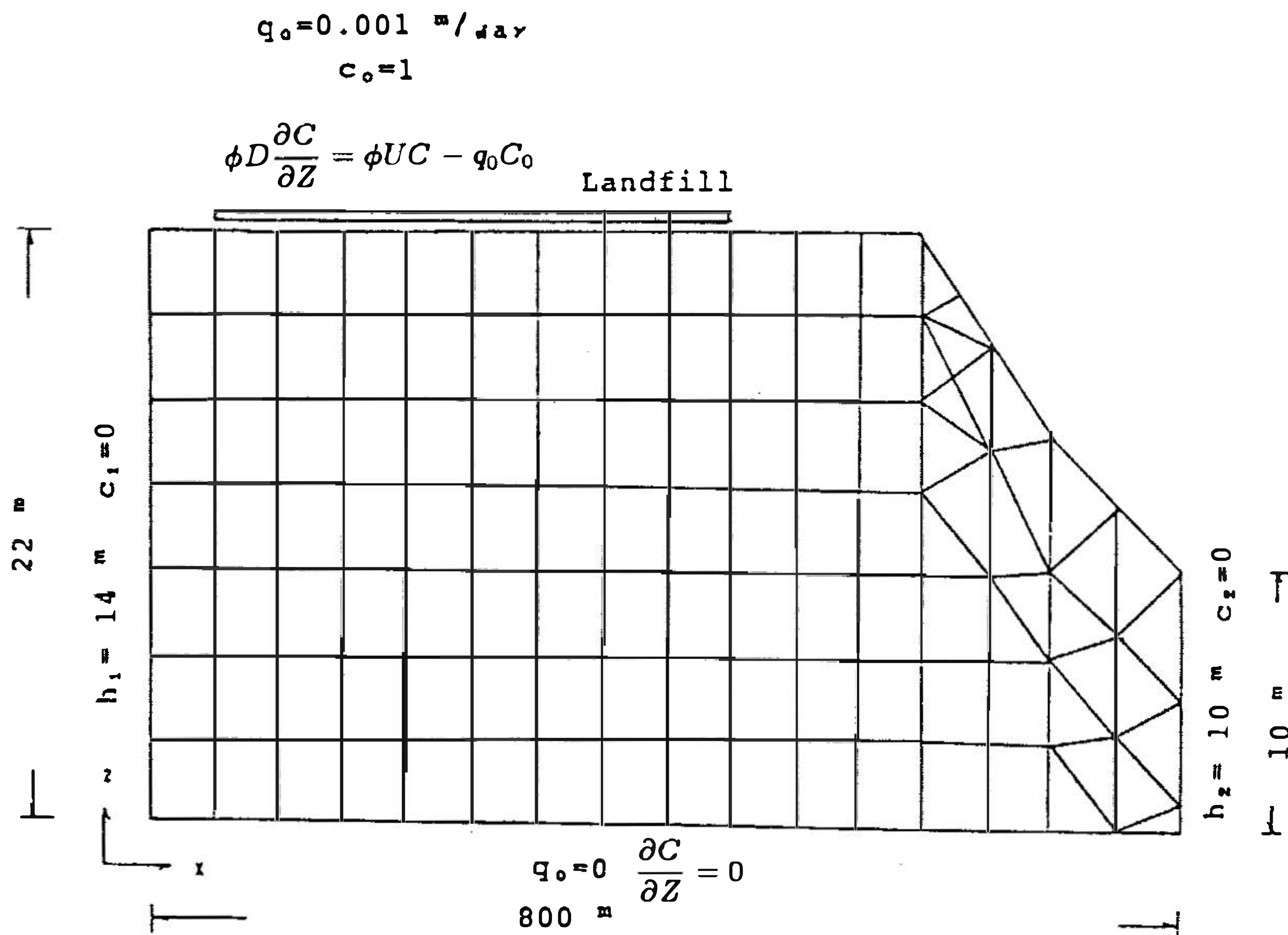


Fig. 10. Boundary conditions and finite element discretizations for modeling leachate transport of the example site.

## 6. DISCUSSION

In the model of density-dependent flow and transport, the change in contaminant concentration may induce the velocity change of fluid flow. If the contaminant solution is considerably denser than the groundwater, the vertical fluid flow velocity increases. Before the solute transport reaches a steady-state, the contaminant concentration changes with time, causing the fluid flow velocity to change with time. Therefore, the solute transport should be considered in terms of an unsteady-state flow field. It is to be noted the fluid flow velocity ( $U_i$ ) in the advection term of equations (9) and (28) is not a constant, i.e.,  $\partial(U_i C)/\partial x_i = U_i(\partial C/\partial x_i) + C(\partial U_i/\partial x_i)$ . However, in general,  $U_i$  is dealt with as a constant (i.e.,  $\partial(U_i C)/\partial x_i = U_i \partial C/\partial x_i$ ) when the density differences are small, and  $\partial U_i/\partial x_i$  can be ignored. This indicates that the change in the contaminant solution does not induce a distinct difference in  $\partial U_i/\partial x_i$ . With the consideration of  $C \partial U_i/\partial x_i$  neglected, the computation time can be reduced without any significant loss of accuracy. However, if the density differences are high ( $\gamma > 0.1$ ),  $U_i$  is not constant in space and, hence,  $\partial U_i/\partial x_i$  cannot be ignored. Otherwise, the simulated results would be subject to significant errors.

Besides the effect of density contrast, the modeling results for Cases 1 and 2 in this research indicate that the transport migration pattern can also be influenced by the hydraulic conductivity ( $K$ ) contrast between the aquifer and aquitard materials, especially for differences of more than two orders of magnitude in hydraulic conductivity. The porosities ( $\phi$ ) are also different for the aquifer and the aquitard lens. Therefore, the values of the fluid flow velocity ( $U_i$ ) in the advection terms of the solute transport equation (i.e., equation (9)) are affected. Accordingly, the concentration distribution and migration pattern is changed. Contaminants travel fast in the aquifer and become slower through the aquitard lens, thereby causing the concentration contours to be distorted, especially at longer transport times of 3 to 6 years.

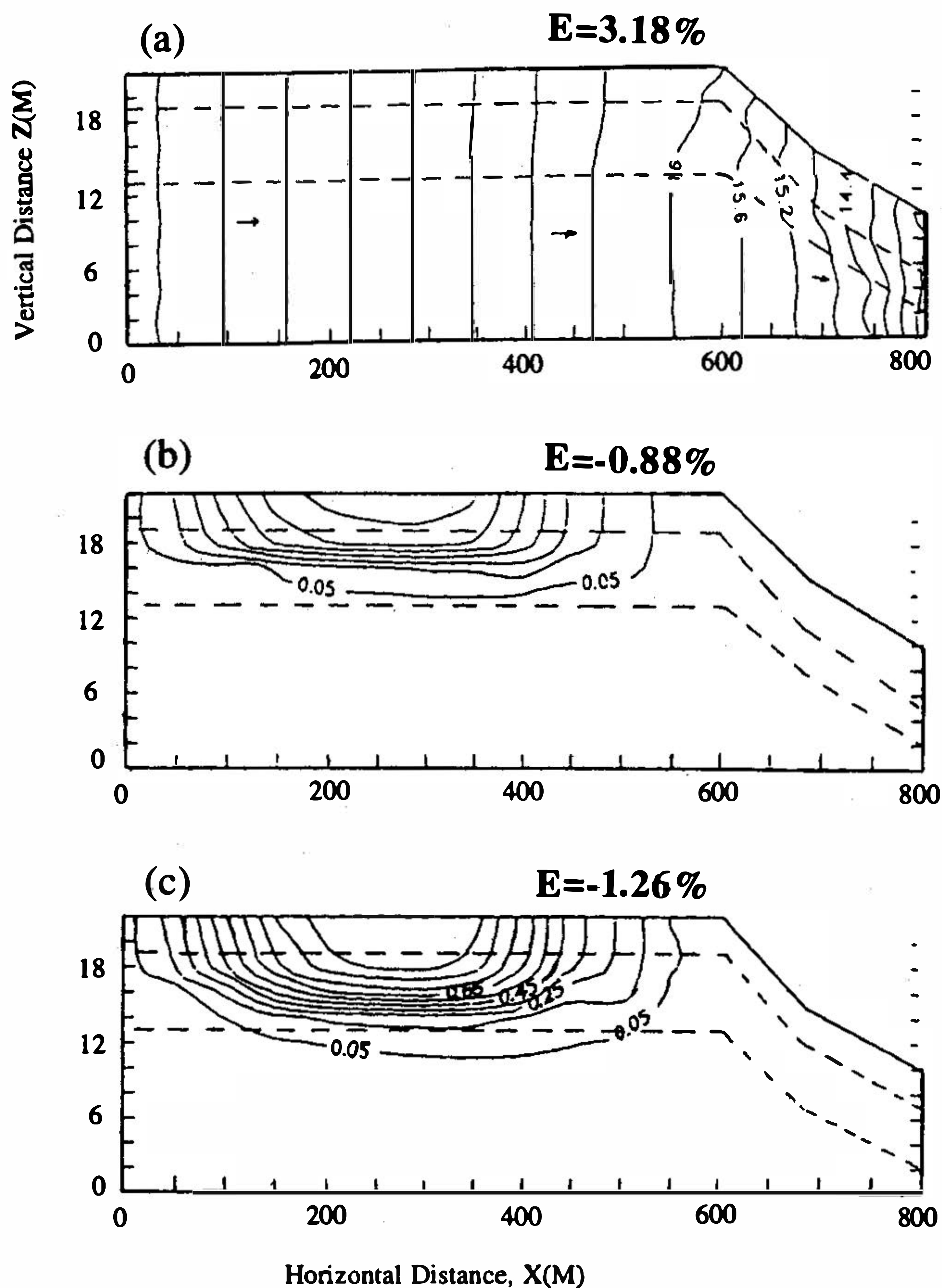


Fig. 11. Modeling leachate transport for the example site: (a) steady-state flow net, (b) concentration distributions after 1000 days and (c) concentration distributions after 2000 days of elapsed time with the density contrast  $\gamma=0.0071$ .

The modeling results for the example site of landfill in this research imply that the transport migration pattern can be affected by the longitudinal dispersivity ( $\alpha_L$ ) and transverse dispersivity ( $\alpha_T$ ). The values of  $\alpha_L$  and  $\alpha_T$  in the aquifers 1 and 2 are greater than those in the aquitard layer. Contaminants can spread to occupy a portion of the flow system many times larger than would be the case in the presence of advection alone. If the transverse dispersivity is very large, contaminants transported along relatively horizontal flow paths can migrate deep into the flow system. Freeze and Cherry (1979) indicated that if dispersivity values are orders of magnitude larger than the values obtained from laboratory experiments, the dispersion exerts a strong influence on the contaminant transport.

From long-term water-quality monitoring, in a real case of a landfill site, McFarlane *et al.* (1983) found that the chemical reaction heat from solid waste decomposition was associated with the leachates and was carried into aquifers. The aquifers then became non-isothermal due to the reaction heat, with a maximum temperature difference of  $5.5^\circ\text{C}$  which can affect the viscosity ( $5.5^\circ\text{C}$  can reduce leachate viscosity by  $10^\circ$ ). However, this research

assumes that the contaminant transport is isothermal with no chemical heat formation during the solid waste decomposition, and therefore, the velocity change in the fluid flow is induced only by the density contrast between the contaminant solution and the groundwater. This velocity change can affect the concentration distribution and migration pattern of the plume in the contaminant transport process.

## 7. CONCLUSIONS

Because the leachate from a landfill site into the groundwater can change the contaminant concentration, there exists a density contrast between the contaminant fluid and the groundwater in the surrounding flow domain. This density contrast can affect the groundwater flow and, consequently, the migration patterns and concentration distribution of contaminant plumes. The density gradients can influence the flow pattern and hence the transport of solutes infiltration from a landfill.

The simulation results in this research are for the problems of density-dependent groundwater flow and transport in homogeneous, anisotropic and inhomogeneous, anisotropic aquifers of a landfill site by means of a Galerkin finite element method. It is shown that if there does not exist a significant density contrast, the contaminant plume spreads in a shallow zone close to the water table; if there is such a contrast, the plume will sink downward into the groundwater flow system, and its migration pattern is significantly changed after a longer transport time of six years. However, the migration pattern is not significantly changed in a shorter time period of one to three years.

The modeling results by Galeati *et al.* (1992) are in good agreement with those by Frind (1982), as shown in Figure 1. The numerical model of Galeati *et al.* (1992) was used to simulate the leachate transport problems including the example site. All showed <5% mass balance errors and it can be concluded that the modeling results can also be applicable to a landfill site.

**Acknowledgements** The authors would like to thank Hund-Der Yeh and Cheng-Haw Lee for their constructive comments. This study was supported by the National Science Council under Grant NSC 80-0421-M006-01.

## REFERENCES

- Batu, V., 1990: A finite element dual mesh method to calculate nodal Darcy velocity in nonhomogeneous and anisotropic aquifers. *Water Resour. Res.*, **20**, 1705-1717.
- Bear, J., 1979: *Hydraulics of Groundwater*. McGraw-Hill, New York, 569pp.
- Bear, J., and A. Verruijt, 1990: *Modeling Groundwater Flow and Pollution*. D. Reidel Publishing Co., Dordrecht, 414pp.
- Childs, K. E., S. B. Upchurch, and B. Ellis, 1974: Sampling of variable waste-migration patterns in groundwater. *Ground Water*, **12**, 369-376.
- Dorgarten, H. W., and C. F. Tsang, 1991: Modeling the density-driven movement of the liquid wastes in deep sloping aquifers. *Ground Water*, **29**, 655-662.
- Freeze, R. A., and J. A. Cherry, 1979: *Groundwater*. Prentice-Hall, New Jersey, 604pp.

- Frind, E. O., 1982: Simulation of long-term transient density-dependent transport in groundwater. *Adv. Water Resour.*, **5**, 73-88.
- Galeati, G., G. Gambolati, and S. P. Neuman, 1992: Coupled and partially coupled Eulerian-Lagrangian model of freshwater-seawater mixing. *Water Resour. Res.*, **28**, 149-165.
- Hassanizadeh, S. M., and T. Leijnse, 1988: On the modeling of brine transport in porous media. *Water Resour. Res.*, **24**, 321-330.
- Henry, H. R., 1964: Effects of dispersion on salt encroachment in coastal aquifers, *Sea Water in Coastal Aquifers. U.S. Geol. Surv. Water Supply Pap.*, **1613-C**, 70-84.
- Huyakorn, P. S., and G. F. Pinder, 1983: *Computational Method in Subsurface Flow*. Academic Press, 437pp.
- Huyakorn, P. S., R. W. Broome, A. G. Kretschek, and J. W. Mercer, 1985: *A Simple and Efficient Flow and Transport Code*. GeoTrans, Inc., 141pp.
- Huyakorn, P. S., P. F. Anderson, J. W. Mercer, and H. O. White, Jr., 1987: Saltwater intrusion in aquifers: Development and testing of a three-dimensional finite element model. *Water Resour. Res.*, **23**, 293-312.
- Konikow, L. F., and J. S. Bredehoeft, 1978: *Computer Model of Two-Dimensional Solute Transport and Dispersion in Groundwater*. Techniques of Water Resources Investigation of the U.S. Geological Survey, U.S. Government Printing Office, Washington, D. C., 90pp.
- Kuiper, K. L. 1983: A numerical procedure for the solution of the steady state variable density groundwater flow equation. *Ground Water*, **19**, 234-240.
- McFarlane, D. S., J. A. Cherry, F. W. Gillham, and E. A. Sudicky, 1983: Migration of contaminations in groundwater at a landfill: A case study 1. Groundwater flow and plume delineation. *J. Hydrol.*, **63**, 1-29.
- Pinder, G. F., and E. O. Frind, 1972: Application of Galerkin's procedure to aquifer analysis. *Water Resour. Res.*, **8**, 108-119.
- Segol, G., G. F. Pinder, and W. G. Gray, 1975: A Galerkin-finite element technique for calculating the transient position of the saltwater front. *Water Resour. Res.*, **11**, 343-347.
- Voss, C. I. and W. R. Souza, 1987: Variable density flow and solute transport simulation of regional aquifers containing a narrow freshwater-saltwater transition zone. *Water Resour. Res.*, **23**, 1851-1866.
- Wang, H. G., and M. P. Anderson, 1983: *Introduction to Groundwater Modeling*. Freeman and Co., San Francisco, 237pp.
- Yeh, G. T., 1981: On the computation of Darcian velocity and mass balance in the finite element modeling of groundwater flow. *Water Resour. Res.*, **17**, 1529-1534.

